HHS Public Access

Author manuscript

Kidney Int. Author manuscript; available in PMC 2018 January 01.

Published in final edited form as:

Kidney Int. 2017 January ; 91(1): 129–143. doi:10.1016/j.kint.2016.07.037.

Human vascular progenitor cells derived from renal arteries are endothelial-like and assist in the repair of injured renal capillary networks

Paul Pang, MSc[1], **Molly Abbott, BSc**[1], **Steven L. Chang, MD, MS**[2], **Malyun Abdi, BSc**[1], **Nikita Chauhan, BSc**[1], **Murti Mistri, BSc**[1], **Joshua Ghofrani**[1], **Quynh-Anh Fucci**[1], **Colleen Walker**[1], **Corey Leonardi, BSc**[1], **Samuel Grady**[1], **Stefan G. Tullius, MD, PhD**[3], **Sayeed Malek**[3], **Sanjaya Kumar, MD**[3], **Graeme Steele**[2], **Adam Kibel, MD**[2], **Benjamin S. Freedman, PhD**[4], **Sushrut S. Waikar, MD, MPH**[1], and **Andrew M. Siedlecki, MD**[1]

[1]Department of Internal Medicine, Brigham and Women's Hospital, Harvard Medical School, 75 Francis St., Boston, Massachusetts, 02115

[2]Urology Division, Department of Surgery, Brigham and Women's Hospital, Harvard Medical School, 75 Francis St., Boston, Massachusetts, 02115

[3]Transplant Surgery Division, Department of Surgery, Brigham and Women's Hospital, Harvard Medical School, 75 Francis St., Boston, Massachusetts, 02115

Washington University, Department of Medicine

Abstract

Vascular progenitor cells show promise for the treatment of microvasculature endothelial injury. We investigated the function of renal artery progenitor cells derived from radical nephrectomy patients, in animal models of acute ischemic and hyperperfusion injuries. Present in human adventitia, CD34positive/CD105negative cells were clonal and expressed transcription factors Sox2/Oct4 as well as surface markers CXCR4 (CD184)/KDR(CD309) consistent with endothelial progenitor cells. Termed renal artery-derived vascular progenitor cells (RAPC), injected cells were associated with decreased serum creatinine after ischemia/reperfusion, reduced albuminuria after hyperperfusion, and improved blood flow in both models. A small population of RAPC integrated with the renal microvasculature following either experimental injury. At a cellular level, RAPC promoted local endothelial migration in co-culture. Profiling of RAPC microRNA identified high levels of miRNA 218; also found at high levels in exosomes isolated from RAPC conditioned media after cell contact for 24 hours. After hydrogen peroxide-induced endothelial injury, RAPC exosomes harbored Robo-1 transcript; a gene known to be regulated by mir218. Such exosomes enhanced endothelial cell migration in culture in the absence of RAPC. Thus, our work shows the

Corresponding author's contact information: Andrew M. Siedlecki, MD, Harvard Institutes of Medicine, 77 Avenue Louis Pasteur, HIM Rm 568B, Boston, MA 02115, Ph 314-809-2879, Fax 617-582-6167, asiedlecki@bwh.harvard.edu.

Disclosures:
All the authors declared no competing interests.

feasibility of pre-emptive pro-angiogenic progenitor cell procurement from a targeted patient population and potential therapeutic use in the form of autologous cell transplantation.

Keywords

acute kidney injury; endothelium; stem cell; hyperfiltration; ischemia reperfusion

INTRODUCTION

Vascular progenitor cells (VPC) are found in extra-marrow sites including human skeletal muscle microvasculature[1], the adult saphenous vein,[2] the adult circulation,[3] and the fetal aorta.[4] As these cells express CD34, a transmembrane sialomucin[5], they have been termed either mesenchymal stem cells or endothelial progenitor cells. Isolation of endothelial progenitor cells centers on the circulating capacity of the cell type.[3, 6] Endothelial progenitor cells have yet to be isolated from discarded tissue and evaluated as a therapeutic for kidney injury.

Endothelial cell injury is central to the pathophysiology of acute renal ischemia/reperfusion injury (IRI) and nephron mass reduction (NMR). During IRI the endothelial cells that compose the peritubular capillaries in the renal cortex and outer medulla are damaged due to oxygen depletion and reactive oxygen species generation.[7–9] NMR results in hyperperfusion and increased shear stress on the endothelial cell surface of the afferent arteriole and glomerulus. Increased glomerular pressure results in albuminuria as described in pre-clinical and clinical studies of NMR.[10, 11]

Renal endothelial cell injury is manifest in the setting of radical nephrectomy. People who donate a kidney for transplantation have an increased risk for renal failure within eight years[12] while half of patients undergoing total nephrectomy as extirpative therapy for renal cell cancer develop kidney disease within 20 months of the procedure.[13] Etiologies include recurrent ischemia/reperfusion and hyperperfusion injury disrupting endothelial function in the kidney microcapillary network.

In this current work we demonstrate that CD34 positive/CD105 negative cells can be isolated from a patient's renal artery at time of radical nephrectomy. This cell population demonstrates endothelial progenitor-like characteristics and integrates into capillaries after acute ischemia/reperfusion injury and nephron mass reduction. Given the risk of kidney disease progression in patients undergoing unilateral nephrectomy, we report for the first time the feasibility of pre-emptive procurement of progenitor cells from the discarded arterial tissue of a targeted patient population with the potential for future therapy in the form of autologous cell transplantation.

RESULTS

Human Renal Arteries Contain Vascular Progenitor Cells that Manifest Endothelial Qualities

Renal artery cross sections were analyzed consecutively. Cell orientation from donor nephrectomies and renal cell cancer nephrectomies were similar. Tissue revealed nucleated $CD34^+$ cells present in the adventitia distinct from $CD34^+$ cells co-localizing with CD105 and CD31 in the intima of the vasa vasorum (Figure 1A,B). $CD34^+$ cells co-localized with CD309 but not with neural/glial antigen 2 (NG2) (Figure 1B). Orientation of CD34+ cells was consistent in tissue sections irrespective of the indication for nephrectomy. The above histologic characterization informed our proceeding analyses.

CD34 protein was detected in consecutive human renal artery tissue by immunoblot technique (Figure 2A[i]). Several cell markers were observed in dissociated tissue sections undergoing surface receptor analysis using flow cytometry (Figure 2A[ii]). We used single-cell sorting technology to isolate a specific cell population from whole-tissue digest expressing the CD34 surface marker in the absence of CD105 (Figure 2B)(n=22). Cells also expressing CD105, a surface marker localizing to differentiated $CD31^+$ endothelial cells,[14, 15] and mesenchymal stromal stem cells,[16] were analyzed separately (data not shown). Selected $CD34^+/CD105^-$ cells were routinely plated in basal media free of epidermal and vascular endothelial growth factors. Mouse-derived $CD34^+/CD105^-$ cells could be isolated from the renal artery (Supplemental Figure 1), however our studies in this report focused on the characterization of human renal artery-derived $CD34^+/CD105^-$ cells.

Cells were evaluated for properties compatible with a progenitor phenotype (Figure 2C). Single $CD34^+/CD105^-$ cells were distributed in an automated fashion to single wells in 96 well plates. Individual cells demonstrated clonality followed by confluency in 94% of total observations (Figure 2C[i]). Cells could be grown to confluency, trypsinized and re-seeded 20+ times. Stellate bodies were observed within 48 hours of culture on fibronectin-coated (0.5microgram /cm^2) sterile plastic plates (Figure 2C[ii]). Cells avidly phagocytosed LDL after 6 hours (Figure 2B[iii]). Endotube formation was observed in matrigel culture (Figure 2C[iv]). Adhesion to fibronectin, lipid phagocytosis, and endotube formation were consistent with a hematopoietic progenitor cell phenotype.[3, 17] Human inducible pluripotent stem cells derived from dermal fibroblasts expressed Sox2 and Oct4 mRNA in levels similar to isolated cells (Figure 2D). RAPC did not express smooth muscle actin however mesenchymal transformation was induced after prolonged exposure to TGF-β1 (Supplemental Figure 2).

Plated cells maintained co-expression of CD309, a marker of endothelial progenitor cells, and CD184 (Figure 3A[i])(n=22). CD14 expression was variable however CD163, expressed by differentiated tissue macrophages,[18] was not present in the selected cell population of interest (Figure 3A[ii]). Cells displayed a differentiated endothelial phenotype after treatment with VEGF for seven days. Monolayers exposed to VEGF expressed surface markers including CD73, CD105, CD202, and CD31 also found on the surface of human endothelial cells (Figure 3B). Endothelial nitric oxide synthase (NOS) was increased 6.9-fold compared to untreated progenitor cells (Figure 3C). eNOS protein levels increased 27.6% following VEGF treatment. vWF protein expression increased 16.1-fold (Figure 3D).

Based on the above results the cells of interest were identified as renal artery-derived vascular endothelial progenitor cells (RAPC) rather than cells of mesenchymal origin.

Renal Artery Derived Progenitor Cells (RAPCs) Integrate In Peritubular Capillaries After Renal Ischemia/Reperfusion Injury

If cells that reside in the adventitia of the renal artery directly affect the renal parenchyma in nature, there must be evidence of cell transit. CMdil cytotracker was microsurgically injected to the adventitia of the mouse renal artery to determine if cell transit occurred during the repair phase following IRI. Five days after IRI, less than five CMdil+ cell per 1,000 total cells was identified in the region of the kidney cortex and outer medulla and two CMdil+ cells per 1000 after ten days (Figure 4). These findings indicated few endogenous adventitial cells of any type migrated from the renal artery to the kidney parenchyma after IRI in a mouse model.

Despite the infrequent event of transmural migration, animals were administered RAPC by intravenous tail injection after IRI to simulate previously successful cell-based treatment approaches.[19, 20] NOD/ShiLtSz-*Prkdc*^{scid} (NOD-SCID) animals underwent kidney ischemia/reperfusion injury (IRI) followed by tail vein injection of human RAPC to assess function in a pre-clinical injury model that did not require immunosuppression. In fixed tissue monoclonal anti-HLA-ABC antibody was used to identify if human cells localized to the mouse kidney after IRI. HLA^{+} cells were then sorted and re-cultured to confirm the monoclonal antibody was binding to the surface of viable human cells and not cellular debris. Whole kidney was digested and HLA+ cells were sorted (n=5) (1.97±1.29%) by flow cytometry, re-cultured and submitted for Combined DNA Index System short tandem repeat polymorphism (STR) analysis (Figure 5). DNA identity was confirmed in each match analysis linking individual cell culture to the associated patient. DNA analysis was also compared to known non-self input (n=5) to confirm the specificity of the technique.

Separately, tissue was processed to study the location of HLA+ cells in the kidney. It has been previously shown that bone marrow-derived mesenchymal stem cells localize to the kidney interstitium after IRI following intravenous injection.[19] We therefore compared RAPC, as a potential cell-based therapy with endothelial-like properties, to MSC following IRI (IRI+RAPC vs IRI+MSC). HLA+ cells were present in histologic sections from IRI +MSC after 5 days (Figure 6A). 2.72-fold more RAPC compared to MSC were present after 5 days, and 4.16-fold more RAPC compared to MSC after 10 days. HLA+ cells were present in IRI+RAPC 10 days after injury localizing to the outer medulla. Few cells were detected in the cortex, inner medulla or papilla. Regional localization of HLA+ cells was confirmed by transducing RAPC with GFP-expressing lentivirus (Supplemental Figure 3 and 4) and injecting cells into animals after IRI as described above. GFP-expressing RAPC were identified three days after injury in peritubular areas containing CD31^{+} cells with highest density in the outer medulla (Supplemental Figure 5). Tissue was re-probed with CD31 antibodies specific for human and mouse epitopes. Cells binding human specific anti-HLA monoclonal antibody were found adjacent to cells binding mouse-specific anti-CD31 antibody (Figure 6B). This finding demonstrated that human cells occupied a

microenvironment shared by mouse endothelial cells. Human $CD31^+$ cells were detected adjacent to mouse $CD31^+$ in greatest number 10 days after IRI (Figure 6B).

Renal Vascular Repair and Renal Function are Affected by RAPC Injection After Ischemia/Reperfusion Injury or After Nephron Mass Reduction

Peritubular capillaries were identified by probing tissue with monoclonal antibody to CD31 estimating capillary density five, ten and twenty days after IRI. All animals survived until each time point. In a separate cohort, 30 day survival rate after IRI in NOD-SCID animals was 91% (n=11). Mean number of patent peritubular capillaries per tubular lumen increased after ten and twenty days in RAPC-treated compared to MSC-treated animals at the same time points (Figure 7A[i]). Capillary density paralleled results obtained by fluorescence microangiography performed twenty days after IRI (Figure 7A[ii]). Renal function was measured by serum creatinine on day 2, 10, and 20. On day 10 and day 20, renal function improved in animals treated with RAPC or MSC compared to animals treated with vehicle. On day 10 renal function improved in RAPC-treated animals compared to MSC-treated animals (Figure 7B). Renal perfusion was measured 20 days after IRI by dynamic MRI. Perfusion increased in animals treated with RAPC compared to animals treated with MSC or vehicle (Figure 7C).

Function of RAPC was assessed in a second model of endothelial injury involving nephron mass reduction (NMR). Animals underwent NMR and followed by treatment with human derived RAPC or MSC. On day 5 and day 10 RAPC were present in glomeruli after injury in greater proportion per total glomeruli (Figure 8A[i]) and in greater number of cells per glomeruli (Figure 8A[ii]) compared to MSC. Serum creatinine was similar in RAPC-treated animals compared to MSC (Figure 7B[i]). Urinary albumin was decreased in RAPC and MSC-treated animals after 10 days, however after 20 days a persistent reduction in microalbuminuria was only observed in the RAPC-treated group (Figure 8B[ii]). There was no significant difference in microalbuminuria between MSC-treated and vehicle-treated animals 20 days after surgery (Figure 8B[ii]). Cortical renal perfusion improved in RAPC-treated animals after 20 days compared to both MSC- and vehicle-treated animals (Figure 8C).

RAPC Encourage Endothelial Cell Migration in Response to Injury

Local migration may play a critical role in the pro-angiogenic effect of RAPC during microcapillary repair after IRI. Local migration of RAPC+EC co-cultures were first studied with a standardized streak test following H_2O_2 –induced injury (Figure 9). Endothelial cells in co-culture treated with H_2O_2 more rapidly repopulated the denuded surface when compared to endothelial cells without GFP^+ RAPC (Figure 9B). Because the GFP^+ population remained numerically small we inferred RAPC influenced endothelial cells in a paracrine fashion. We proceeded to evaluate the significance of microRNA patterning in RAPC because of the well-known modulatory effect of microRNA in various cell types of the vascular system.[21, 22] We compared miRNA microarray patterns of non-stimulated RAPC to microarrays available in the NCBI-sponsored Gene Expression Omnibus (GEO) database including human endothelial progenitor cells (EPC), human umbilical vein endothelial cells (HUVEC) and human bone marrow-derived mesenchymal stem cells

(MSC). RAPC miRNA patterning most closely correlated with miRNA expressed in EPC (ρ=0.67, CI 0.54–0.79; p<0.01) (Figure 10).[23–25] mir-218 was among 14 miRNA present exclusively in EPC and RAPC microarrays (Figure 10, grey box).

We measured mir-218 transcript in several cell types. RAPC culture expressed mir-218 2.4-fold higher than human endothelial cell culture, 11.1-fold compared to human vascular smooth muscle cell culture, 9.1-fold compared to human mesenchymal stem cell culture and >50-fold compared to human inducible pluripotent stem cell culture when quantitated by RT-PCR (Figure 10B). In vitro mir-218 expression in RAPC was suppressed using LNA-mir-218. A corresponding increase in Robo-1 protein expression was observed by immunoblot (Figure 10C). Functional susceptibility of RAPC to mir-218 inhibition was confirmed with cell migration studies that demonstrated sensitivity of RAPC to mir-218 inhibition significantly greater than endothelial cells (Figure 10D).

Above we determined that endogenous migration of RAPC from the adventitia of the renal artery to the renal parenchyma was limited (Figure 4). However we additionally identified exosomes that contained mir218 transcript in the supernatant of RAPC culture (Figure 11A). Under maintenance conditions, exosomes from RAPC contained mir218. Following oxidant stress, exosomal mir-218 levels were diminished (Figure 11B[i]) while exosomal Robo1 mRNA levels were enriched (Figure 11B[ii]). Exosomes isolated from RAPC treated with LNA-mir218 also contained increased Robo1 mRNA transcript (Figure 11B). Exosomes from conditioned RAPC were then added to injured endothelial cells alone and migration increased in comparison to cells treated with exosomes from RAPC cultured under maintenance conditions (Figure 11C).

DISCUSSION

We report on the discovery of a cell population in human renal arterial adventitia that not only exhibits progenitor cell qualities with the capacity to differentiate into human endothelial cells in a murine kidney model, but also contribute to accelerated recovery of peritubular capillary density following intravenous injection. Our studies support the conclusion that $CD34^+$ and $CD105^-$ cell selection was effective to isolate an endothelial progenitor cell subtype whereas expression of CD34 and CD105 was most consistent with a differentiated endothelial cell[14, 26] or one of mesenchymal origin.[2]

To meet the definition of a progenitor, selected cells were evaluated with both qualitative and functional assays. RAPC exhibited clonality and expressed Sox2 and Oct4. Sox2 and Oct4 levels were comparable to human inducible pluripotent stem cells. RAPC could be cultured and were characterized positively by CD309 and CD184 surface expression and negatively by low expression of CD31, CD105, and CD73. CD309 co-localized to $CD34^+$ cells in the adventitia of each human renal artery we analyzed. Werner and colleagues used CD309 to identify circulating human endothelial progenitor cells.[27] Walter and colleagues showed CD184 was critical to endothelial progenitor cell migration.[28] In aggregate our studies show RAPC to be characterized as progenitor cells that can differentiate into endothelial cells that express CD73[29, 30], CD 105, CD31, exhibit endotube formation, NOS activity and express high levels of vWF.[3]

We compared RAPC therapy to MSC therapy because MSC were reported to have an effect in the setting of kidney-specific IRI. Capillary rarefaction and tubular epithelial cell damage following kidney-specific IRI has been reduced by MSC therapy in pre-clinical models.[31, 32] However most MSC, being of stromal origin, have infrequently been identified to display endothelial-like properties.[33] Our experiments demonstrated that RAPC had greater beneficial effect on models of kidney-specific endothelial cell injury.

We first characterized RAPC function after IRI. Although progenitor cell density decreased after 10 and 20 days others have speculated that the vital period of progenitor cell activity is the first week following kidney injury.[20, 34] Serum creatinine improved more quickly in animals treated with RAPC. Blood perfusion was increased in RAPC-treated animals and coincided with an increase in capillary density. MRI results and corresponding histology inferred that differences in kidney perfusion may anticipate chronic kidney injury despite unrevealing serum creatinine levels.[8]

Following NMR, RAPC affected albuminuria and renal perfusion while renal function was unchanged. Histologic analysis showed RAPC localizing to the glomerulus in higher density compared to peritubular capillary localization of RAPC in the IRI model. Increased albuminuria after 10 days was consistent with glomerular injury associated with the renin-angiotensin system activation and subsequent glomerular hyperfiltration.[35, 36] Albuminuria was improved in RAPC- and MSC-treated animals compared to vehicle at 10 days with persistent effect in RAPC-treated after 20 days. Renal perfusion was also improved in RAPC compared to MSC after 20 days. The mechanism of RAPC function in NMR is unclear but localization of RAPC to the glomerulus, reduction in albuminuria, and improvement of renal perfusion implicates a normalization of flow dynamics in the microvasculature due to accelerated endothelial repair.

The role of mir218 in angiogenesis reinforced the potential for RAPC to promote an endothelial program and offered a potential mechanism by which RAPC promoted endothelial repair.[37–39] Microrray results were confirmed by RT-PCR demonstrating that vitro RAPC expressed relatively high levels of mir218 compared to other cell types interrogated. This finding was consistent with a sedentary phenotype that could be manipulated using anti-mir218 conditioning. This was further demonstrated by increased Robo-1 protein expression when mir218 was inhibited. These findings were consistent with others that have shown Robo-1 is regulated by mir-218 expression and that upregulation of Robo-1 is linked with endothelial migration.[37]

We then made the critical discovery that mir-218 and Robo-1 mRNA are differentially expressed by exosomes derived from RAPC. Following treatment of injured endothelial cells with RAPC-derived exosomes, endothelial migration improved. LNA-mir218 treatment further emphasized how RAPC may be conditioned prior to injection to enhance Robo-1 transmission and stimulate a reparative phenotype via exosome delivery.

Our study is limited by anatomic variation in the mouse renal artery compared to the human renal artery. Namely, the mouse renal artery contains no vasa vasorum since the vascular thickness of murine renal arteries does not necessitate this for oxygen delivery. However, we

demonstrated that mouse-derived CD34+/CD105− cells can be isolated from dissociated renal artery tissue and cultured in vitro. This infers a murine analogue to human RAPC which deserves further investigation in future studies.

Conclusion

We describe a unique progenitor cell population derived from discarded renal artery tissue of patients undergoing radical nephrectomy. RAPC show the capacity to differentiate into endothelial cells and have functional benefit in two models of renal microvascular injury. Mir218 is a critical modulator of RAPC function which we validated in both isolated human tissue culture and pre-clinical animal models. Our discoveries have direct clinical application. Select patients undergoing radical nephrectomy are at risk of progressive decline in renal function. We offer a conceptual framework in which autologous progenitor cells can be utilized for patients with an immediate therapeutic need.

CONCISE METHODS

Human Renal Artery Procurement

Written consent was obtained from all participating patients prior to tissue procurement. Renal arteries were procured in the operating room by means of the Brigham and Women's Hospital Tissue and Blood Repository service.

$CD34^{+}/CD105^{-}$ Cell Isolation

Human renal artery tissue was minced under sterile technique then placed in FBS-free Endothelial Basal Media-2 (EBM2) media (Lonza, Inc) and digested with collagenase type II (0.5mg/mL) and collagenase type IV (0.5mg/mL) (Thermo Scientific Fisher, Inc) for 25 minutes at 37C. Whole tissue was then filtered through a 70micron filter. Cell pellet was generated and resuspended in FACS buffer containing human anti-CD34 antibody labelled with APC and human anti-CD105 antibody labelled with FITC. Cell Sorting was performed with a BD FACSAria sorter special order system using FACSDiva software version 6.1.2 Cells were plated on a $3.2cm^2$ sterile plastic surface and cultured in EBM2 (Lonza Inc) containing basic fibroblast growth factor, ascorbic acid, insulin-like growth factor, hydrocortisone, and 5% fetal bovine serum without epidermal growth factor (EGF) or vascular endothelial growth factor (VEGF). Using similar technique mouse renal artery-derived CD34+/CD105− cells were isolated (Supplemental Figure 1).

Murine 30 Minute Bilateral Renal Ischemia/reperfusion Injury Model

All research involving the use of mice were performed in strict accordance with protocols approved by the Animal Studies Committee of Harvard Medical School. Ischemia/reperfusion injury was performed as we previously described.[40, 41]

Murine Nephron mass reduction (NMR) Model

NMR was performed using a technique that we and others have described previously.[42, 43] The surgery required two stages. Unilateral nephrectomy was performed followed by removal of the upper and lower pole of the contralateral kidney one week after the first

surgery. Absorbable gelatin (Pfizer, Inc.) was applied to the cortical incisions to achieve hemostasis. The model maintained elevated serum creatinine (0.18±0.01mg/dL) eight weeks after injury (Supplemental Figure 6).

Cell Culture Preparation and Injection in Animal Models of Kidney Injury

Human RAPC were grown to 80–90% confluency, then harvested and quantified by hemoctyometry. 1.0×10^6 cells were re-suspended in sterile normal saline and administered through the tail vein. Human bone-marrow derived MSC were prepared using the same growth and quantification parameters.

Renal Perfusion by Dynamic Contrast-Enhanced Magnentic Resonance Imaging

Studies were performed as previously reported.[41, 44] Imaging protocol parameters included echo time, 1085ms; repetition time 2170ms; excitation pulse angle, 60; flip angle, 30; FOV 5×4 cm; matrix size 128×96; slice thickness, 1.5mm. All images were obtained in the transverse plane.

Exosome isolation

Exosomes were isolated as previously described.[45] Briefly, RAPC reaching 70–80% confluency were incubated with fresh media for 24 hours. Media was removed under sterile conditions, and centrifuged at 10,000g for 30 minutes, then passed through a 0.22 micrometer filter and combined with Exoquick (SBI, Inc.) per the manufacturer's instructions. Exosome-rich isolates were enriched by ultracentrifugation for 70 minutes at 100,000g. Exosome pellets were then re-suspended in Trizol or media or PBS according to the experimental condition. For migration studies exosomal RNA concentrations were measured with a NanoDrop 2000c spectrophotometer (Thermo Scientific, Inc.).

Cell migration assay

Human endothelial cell and human RAPC co-culture was generated as described above. Cells were then transferred to $3.2cm^2$ wells in a 10:1 ratio, 56,000 (EC) : 5,600 (RAPC). A linear streak of cells approximately 700micrometers in width was denuded under sterile conditions. Cell migration was monitored for twenty hours using a Nikon ECLIPSE Ti Inverted Research Microscope. Live cells were kept in a humidified chamber kept at constant temperature (37C) with continuous 6% CO_2 supplementation surrounding the microscope housing. Rate change of cell movement was calculated by obtaining digital photomicrographs every 15 minutes. Images were processed using NIS-Elements Imaging/ analysis Software (Nikon, Inc.). Cells conditioned with H_2O_2 were treated with 2.5μM H_2O_2 for 6 hours and fresh media was then exchanged. Single cell types were plated and transfected with mir218-LNA or scrambled-LNA. Streak testing was performed as described above. Streaking testing of cells treated with exosome isolates was performed in 96-well plates with RNA concentration of 1ng per microliter of EC media.

Statistical analysis

SPSS v22 (IBM, Inc.) software was used for all calculations. Experimental conditions were evaluated for significance using analysis of variance (ANOVA) in pair-wise group

comparison among multiple groups along with the Bonferroni correction method. Student's T-test was used to evaluate for significance between two groups. Log-rank testing (Mantel-Cox) was used to compare survival between two groups. All values represent a condition's mean value ± standard deviation.

Supplementary Material

Refer to Web version on PubMed Central for supplementary material.

Acknowledgments

Human inducible pluripotent stem cells were provided as a generous gift from Dr. Albert Lam. Lentivirus was provided as a generous gift from Dr. Yiling Qui.

Funding Sources: This work was supported by NIH grant K08DK089002 (A.M.S), U01DK104308 (S.S.W.), Brigham and Women's Hospital Faculty Career Development Award (A.M.S.), University of Alabama at Birmingham/University of California-San Diego O'Brien Core Center for Acute Kidney Injury Research (NIH P30 DK 079337).

References

1. Crisan M, Yap S, Casteilla L, Chen CW, Corselli M, Park TS, Andriolo G, Sun B, Zheng B, Zhang L, Norotte C, Teng PN, Traas J, Schugar R, Deasy BM, Badylak S, Buhring HJ, Giacobino JP, Lazzari L, Huard J, Peault B. A perivascular origin for mesenchymal stem cells in multiple human organs. Cell stem cell. 2008; 3:301–313. [PubMed: 18786417]
2. Campagnolo P, Cesselli D, Al Haj Zen A, Beltrami AP, Krankel N, Katare R, Angelini G, Emanueli C, Madeddu P. Human adult vena saphena contains perivascular progenitor cells endowed with clonogenic and proangiogenic potential. Circulation. 2010; 121:1735–1745. [PubMed: 20368523]
3. Asahara T, Murohara T, Sullivan A, Silver M, van der Zee R, Li T, Witzenbichler B, Schatteman G, Isner JM. Isolation of putative progenitor endothelial cells for angiogenesis. Science. 1997; 275:964–967. [PubMed: 9020076]
4. Invernici G, Emanueli C, Madeddu P, Cristini S, Gadau S, Benetti A, Ciusani E, Stassi G, Siragusa M, Nicosia R, Peschle C, Fascio U, Colombo A, Rizzuti T, Parati E, Alessandri G. Human fetal aorta contains vascular progenitor cells capable of inducing vasculogenesis, angiogenesis, and myogenesis in vitro and in a murine model of peripheral ischemia. The American journal of pathology. 2007; 170:1879–1892. [PubMed: 17525256]
5. Wood HB, May G, Healy L, Enver T, Morriss-Kay GM. CD34 expression patterns during early mouse development are related to modes of blood vessel formation and reveal additional sites of hematopoiesis. Blood. 1997; 90:2300–2311. [PubMed: 9310481]
6. Kawamoto A, Katayama M, Handa N, Kinoshita M, Takano H, Horii M, Sadamoto K, Yokoyama A, Yamanaka T, Onodera R, Kuroda A, Baba R, Kaneko Y, Tsukie T, Kurimoto Y, Okada Y, Kihara Y, Morioka S, Fukushima M, Asahara T. Intramuscular transplantation of G-CSF-mobilized CD34(+) cells in patients with critical limb ischemia: a phase I/IIa, multicenter, single-blinded, dose-escalation clinical trial. Stem Cells. 2009; 27:2857–2864. [PubMed: 19711453]
7. Bonventre JV, Yang L. Cellular pathophysiology of ischemic acute kidney injury. The Journal of clinical investigation. 2011; 121:4210–4221. [PubMed: 22045571]
8. Kramann R, Tanaka M, Humphreys BD. Fluorescence microangiography for quantitative assessment of peritubular capillary changes after AKI in mice. Journal of the American Society of Nephrology : JASN. 2014; 25:1924–1931. [PubMed: 24652794]
9. Siedlecki A, Irish W, Brennan DC. Delayed graft function in the kidney transplant. American journal of transplantation : official journal of the American Society of Transplantation and the American Society of Transplant Surgeons. 2011; 11:2279–2296.

10. Hostetter TH, Olson JL, Rennke HG, Venkatachalam MA, Brenner BM. Hyperfiltration in remnant nephrons: a potentially adverse response to renal ablation. Journal of the American Society of Nephrology : JASN. 2001; 12:1315–1325. [PubMed: 11373357]
11. Dekkers IA, Blijdorp K, Cransberg K, Pluijm SM, Pieters R, Neggers SJ, van den Heuvel-Eibrink MM. Long-term nephrotoxicity in adult survivors of childhood cancer. Clinical journal of the American Society of Nephrology : CJASN. 2013; 8:922–929. [PubMed: 23411430]
12. Muzaale AD, Massie AB, Wang MC, Montgomery RA, McBride MA, Wainright JL, Segev DL. Risk of end-stage renal disease following live kidney donation. JAMA : the journal of the American Medical Association. 2014; 311:579–586. [PubMed: 24519297]
13. Huang WC, Levey AS, Serio AM, Snyder M, Vickers AJ, Raj GV, Scardino PT, Russo P. Chronic kidney disease after nephrectomy in patients with renal cortical tumours: a retrospective cohort study. The lancet oncology. 2006; 7:735–740. [PubMed: 16945768]
14. Li C, Issa R, Kumar P, Hampson IN, Lopez-Novoa JM, Bernabeu C, Kumar S. CD105 prevents apoptosis in hypoxic endothelial cells. Journal of cell science. 2003; 116:2677–2685. [PubMed: 12746487]
15. Anderberg C, Cunha SI, Zhai Z, Cortez E, Pardali E, Johnson JR, Franco M, Paez-Ribes M, Cordiner R, Fuxe J, Johansson BR, Goumans MJ, Casanovas O, ten Dijke P, Arthur HM, Pietras K. Deficiency for endoglin in tumor vasculature weakens the endothelial barrier to metastatic dissemination. The Journal of experimental medicine. 2013; 210:563–579. [PubMed: 23401487]
16. Dominici M, Le Blanc K, Mueller I, Slaper-Cortenbach I, Marini F, Krause D, Deans R, Keating A, Prockop D, Horwitz E. Minimal criteria for defining multipotent mesenchymal stromal cells. The International Society for Cellular Therapy position statement. Cytotherapy. 2006; 8:315–317. [PubMed: 16923606]
17. Nagaya N, Kangawa K, Kanda M, Uematsu M, Horio T, Fukuyama N, Hino J, Harada-Shiba M, Okumura H, Tabata Y, Mochizuki N, Chiba Y, Nishioka K, Miyatake K, Asahara T, Hara H, Mori H. Hybrid cell-gene therapy for pulmonary hypertension based on phagocytosing action of endothelial progenitor cells. Circulation. 2003; 108:889–895. [PubMed: 12835224]
18. Fabriek BO, van Bruggen R, Deng DM, Ligtenberg AJ, Nazmi K, Schornagel K, Vloet RP, Dijkstra CD, van den Berg TK. The macrophage scavenger receptor CD163 functions as an innate immune sensor for bacteria. Blood. 2009; 113:887–892. [PubMed: 18849484]
19. Duffield JS, Park KM, Hsiao LL, Kelley VR, Scadden DT, Ichimura T, Bonventre JV. Restoration of tubular epithelial cells during repair of the postischemic kidney occurs independently of bone marrow-derived stem cells. The Journal of clinical investigation. 2005; 115:1743–1755. [PubMed: 16007251]
20. Li B, Cohen A, Hudson TE, Motlagh D, Amrani DL, Duffield JS. Mobilized human hematopoietic stem/progenitor cells promote kidney repair after ischemia/reperfusion injury. Circulation. 2010; 121:2211–2220. [PubMed: 20458011]
21. Abdellatif M. Differential expression of microRNAs in different disease states. Circulation research. 2012; 110:638–650. [PubMed: 22343558]
22. Creemers EE, Tijsen AJ, Pinto YM. Circulating microRNAs: novel biomarkers and extracellular communicators in cardiovascular disease? Circulation research. 2012; 110:483–495. [PubMed: 22302755]
23. O'Toole TE, Abplanalp W, Li X, Cooper N, Conklin DJ, Haberzettl P, Bhatnagar A. Acrolein decreases endothelial cell migration and insulin sensitivity through induction of let-7a. Toxicological sciences : an official journal of the Society of Toxicology. 2014; 140:271–282. [PubMed: 24812010]
24. Wang HW, Huang TS, Lo HH, Huang PH, Lin CC, Chang SJ, Liao KH, Tsai CH, Chan CH, Tsai CF, Cheng YC, Chiu YL, Tsai TN, Cheng CC, Cheng SM. Deficiency of the microRNA-31-microRNA-720 pathway in the plasma and endothelial progenitor cells from patients with coronary artery disease. Arteriosclerosis, thrombosis, and vascular biology. 2014; 34:857–869.
25. Reagan MR, Mishima Y, Glavey SV, Zhang Y, Manier S, Lu ZN, Memarzadeh M, Sacco A, Aljawai Y, Shi J, Tai YT, Ready JE, Kaplan DL, Roccaro AM, Ghobrial IM. Investigating osteogenic differentiation in multiple myeloma using a novel 3D bone marrow niche model. Blood. 2014; 124:3250–3259. [PubMed: 25205118]

26. Middleton J, Americh L, Gayon R, Julien D, Mansat M, Mansat P, Anract P, Cantagrel A, Cattan P, Reimund JM, Aguilar L, Amalric F, Girard JP. A comparative study of endothelial cell markers expressed in chronically inflamed human tissues: MECA-79, Duffy antigen receptor for chemokines, von Willebrand factor, CD31, CD34, CD105 and CD146. The Journal of pathology. 2005; 206:260–268. [PubMed: 15887283]
27. Werner N, Kosiol S, Schiegl T, Ahlers P, Walenta K, Link A, Bohm M, Nickenig G. Circulating endothelial progenitor cells and cardiovascular outcomes. The New England journal of medicine. 2005; 353:999–1007. [PubMed: 16148285]
28. Walter DH, Haendeler J, Reinhold J, Rochwalsky U, Seeger F, Honold J, Hoffmann J, Urbich C, Lehmann R, Arenzana-Seisdesdos F, Aicher A, Heeschen C, Fichtlscherer S, Zeiher AM, Dimmeler S. Impaired CXCR4 signaling contributes to the reduced neovascularization capacity of endothelial progenitor cells from patients with coronary artery disease. Circulation research. 2005; 97:1142–1151. [PubMed: 16254213]
29. Zernecke A, Bidzhekov K, Ozuyaman B, Fraemohs L, Liehn EA, Luscher-Firzlaff JM, Luscher B, Schrader J, Weber C. CD73/ecto-5'-nucleotidase protects against vascular inflammation and neointima formation. Circulation. 2006; 113:2120–2127. [PubMed: 16636171]
30. Bellingan G, Maksimow M, Howell DC, Stotz M, Beale R, Beatty M, Walsh T, Binning A, Davidson A, Kuper M, Shah S, Cooper J, Waris M, Yegutkin GG, Jalkanen J, Salmi M, Piippo I, Jalkanen M, Montgomery H, Jalkanen S. The effect of intravenous interferon-beta-1a (FP-1201) on lung CD73 expression and on acute respiratory distress syndrome mortality: an open-label study. The Lancet Respiratory medicine. 2014; 2:98–107. [PubMed: 24503265]
31. Xing L, Cui R, Peng L, Ma J, Chen X, Xie RJ, Li B. Mesenchymal stem cells, not conditioned medium, contribute to kidney repair after ischemia-reperfusion injury. Stem cell research & therapy. 2014; 5:101. [PubMed: 25145540]
32. Chen Y, Qian H, Zhu W, Zhang X, Yan Y, Ye S, Peng X, Li W, Xu W. Hepatocyte growth factor modification promotes the amelioration effects of human umbilical cord mesenchymal stem cells on rat acute kidney injury. Stem cells and development. 2011; 20:103–113. [PubMed: 20446811]
33. Anjos-Afonso F, Bonnet D. Nonhematopoietic/endothelial SSEA-1+ cells define the most primitive progenitors in the adult murine bone marrow mesenchymal compartment. Blood. 2007; 109:1298–1306. [PubMed: 17003364]
34. Burks SR, Nguyen BA, Tebebi PA, Kim SJ, Bresler MN, Ziadloo A, Street JM, Yuen PS, Star RA, Frank JA. Pulsed focused ultrasound pretreatment improves mesenchymal stromal cell efficacy in preventing and rescuing established acute kidney injury in mice. Stem Cells. 2015; 33:1241–1253. [PubMed: 25640064]
35. Hostetter TH, Olson JL, Rennke HG, Venkatachalam MA, Brenner BM. Hyperfiltration in remnant nephrons: a potentially adverse response to renal ablation. The American journal of physiology. 1981; 241:F85–F93. [PubMed: 7246778]
36. Lafayette RA, Mayer G, Park SK, Meyer TW. Angiotensin II receptor blockade limits glomerular injury in rats with reduced renal mass. The Journal of clinical investigation. 1992; 90:766–771. [PubMed: 1522231]
37. Small EM, Sutherland LB, Rajagopalan KN, Wang S, Olson EN. MicroRNA-218 regulates vascular patterning by modulation of Slit-Robo signaling. Circulation research. 2010; 107:1336–1344. [PubMed: 20947829]
38. Mathew LK, Skuli N, Mucaj V, Lee SS, Zinn PO, Sathyan P, Imtiyaz HZ, Zhang Z, Davuluri RV, Rao S, Venneti S, Lal P, Lathia JD, Rich JN, Keith B, Minn AJ, Simon MC. miR-218 opposes a critical RTK-HIF pathway in mesenchymal glioblastoma. Proceedings of the National Academy of Sciences of the United States of America. 2014; 111:291–296. [PubMed: 24368849]
39. Alajez NM, Lenarduzzi M, Ito E, Hui AB, Shi W, Bruce J, Yue S, Huang SH, Xu W, Waldron J, O'Sullivan B, Liu FF. MiR-218 suppresses nasopharyngeal cancer progression through downregulation of survivin and the SLIT2-ROBO1 pathway. Cancer research. 2011; 71:2381–2391. [PubMed: 21385904]
40. Siedlecki AM, Jin X, Thomas W, Hruska KA, Muslin AJ. RGS4, a GTPase activator, improves renal function in ischemia-reperfusion injury. Kidney international. 2011; 80:263–271. [PubMed: 21412219]

41. Pang P, Jin X, Proctor BM, Farley M, Roy N, Chin MS, von Andrian UH, Vollmann E, Perro M, Hoffman RJ, Chung J, Chauhan N, Mistri M, Muslin AJ, Bonventre JV, Siedlecki AM. RGS4 inhibits angiotensin II signaling and macrophage localization during renal reperfusion injury independent of vasospasm. Kidney international. 2015; 87:771–783. [PubMed: 25469849]

42. Kramann R, Schneider RK, DiRocco DP, Machado F, Fleig S, Bondzie PA, Henderson JM, Ebert BL, Humphreys BD. Perivascular Gli1+ progenitors are key contributors to injury-induced organ fibrosis. Cell stem cell. 2015; 16:51–66. [PubMed: 25465115]

43. Siedlecki AM, Jin X, Muslin AJ. Uremic cardiac hypertrophy is reversed by rapamycin but not by lowering of blood pressure. Kidney international. 2009; 75:800–808. [PubMed: 19165175]

44. Siedlecki A, Anderson JR, Jin X, Garbow JR, Lupu TS, Muslin AJ. RGS4 controls renal blood flow and inhibits cyclosporine-mediated nephrotoxicity. American journal of transplantation : official journal of the American Society of Transplantation and the American Society of Transplant Surgeons. 2010; 10:231–241.

45. Roccaro AM, Sacco A, Maiso P, Azab AK, Tai YT, Reagan M, Azab F, Flores LM, Campigotto F, Weller E, Anderson KC, Scadden DT, Ghobrial IM. BM mesenchymal stromal cell-derived exosomes facilitate multiple myeloma progression. The Journal of clinical investigation. 2013; 123:1542–1555. [PubMed: 23454749]

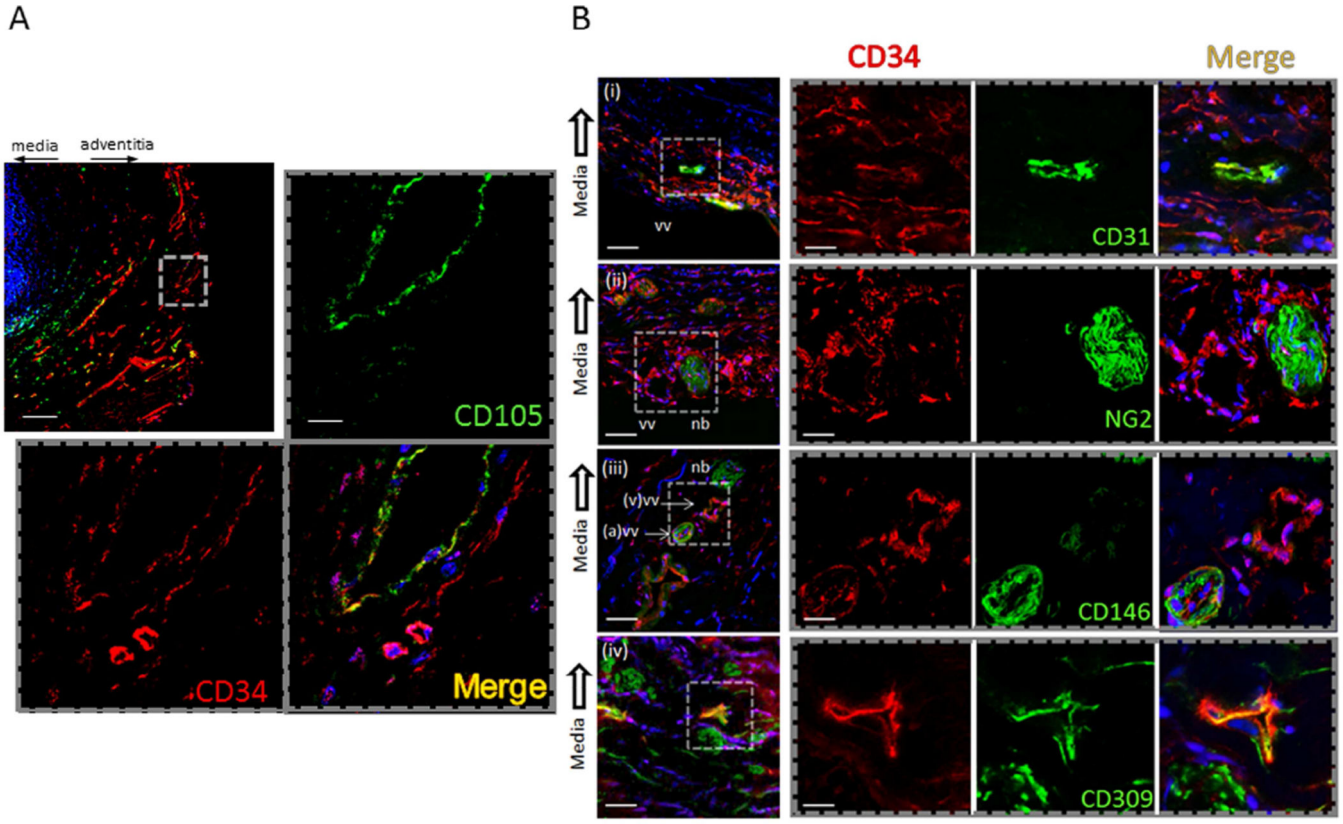

Figure 1.

Histologic distribution of CD34 in the human renal artery. (A) Representative photomicrograph (n=14) of monoclonal antibody probes for CD34 and CD105. CD34 and CD105 probes localize to the adventitia (top left) (scale bar= 250micrometers). CD105 distributes to nucleated cells in the intima of the vasa vasorum, (hashed line inset). CD34 localizes to nucleated cells in adjacent stroma of the adventitia (scale bar=20micrometers). (B) Differential localization of $CD34^+$ cells proximate to the vasa vasorum of the adventitia. (black arrow, toward medial layer in all photomicrographs) (i) $CD31^+$ and $CD34^+$ nucleated cells are present in the intima of the vasa vasorum. $CD34^+$ /$CD31^-$ cells are found in the adjacent stroma (low power scale bar=50 micrometers; high power scale bar=20micrometers). (ii) neural/glial antigen 2 (NG2) displays in adjacent nerve bundles (nb) distinct from CD34+ cells composing vasa vasorum (vv) (low power scale bar=50micrometers; high power scale bar=25micrometers). (iii) $CD146^+$ co-localizes with $CD34^+$ in the arterial vasa vasorum (*a*) distinct from the venous (*v*) vasa vasorum. (iv) $CD34^+$ co-localizes with cells that display $CD309^+$ (low power scale bar=25micrometers; high power scale bar=10micrometers).

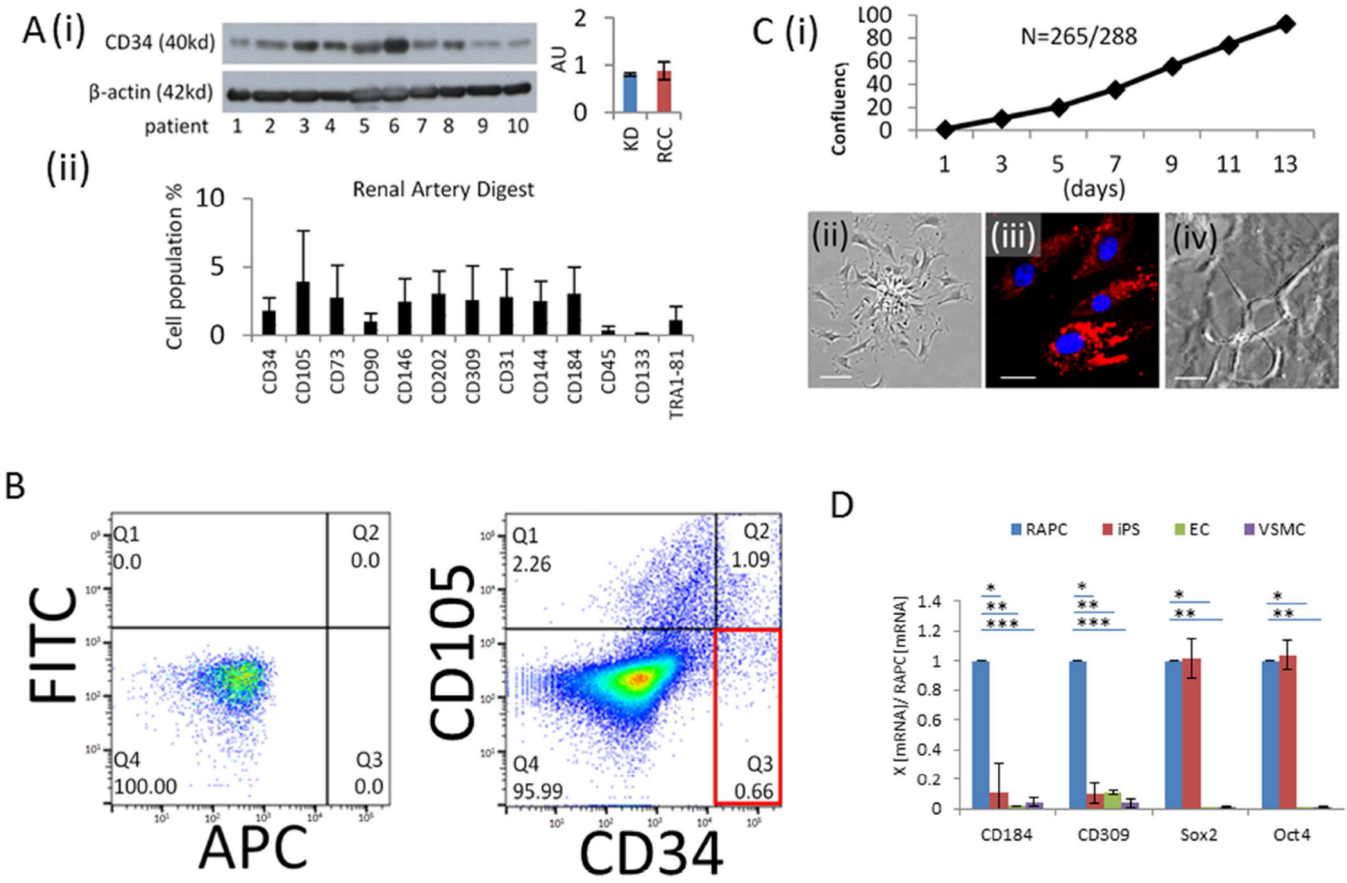

Figure 2.

Characterization of RAPC derived from human renal artery tissue. (A)[i] Representative immunoblot of human renal artery tissue probed for monoclonal anti-human CD34 antibody normalized to beta-actin tissue content. Indication for nephrectomy included living donor kidney donation (lane 1–3) and renal cell cancer (lane 4–10) (relative intensity, 0.80±0.032 vs 0.88±0.19, respectively (p=NS), [ii] Flow cytometry of whole digest (n=26), CD34 (1.8 ± 1.0 %), CD105 (3.9 ± 3.7), CD73 (2.8 ± 2.4), CD90 (1.0 ± 0.6), CD146 (2.4±1.8), CD202 (3.1 ± 1.6), CD309 (2.6 ± 2.5), CD31 (2.8 ± 2.0 %), CD144 (2.5 ± 1.5), CD184 (3.1±1.9), CD45 (0.4 ± 0.3), CD133 (0±0), TR181 (1.1 ± 1.0), (B) $CD34^{+}$ /$CD105^{-}$ cells sorted(%), FITC/APC control (cell count=10,000), $CD34^{+}$/$CD105^{-}$ (0.66±0.47), $CD34^{+}$/$CD105^{+}$ (1.09±0.42), $CD34^{-}$/$CD105^{+}$ (2.26±1.00) (n=22). (C)[i] Individually sorted $CD34^{+}$/$CD105^{-}$ cells distributed into single wells of a 96-well plate, cultured in basal media, and monitored daily for colony formation and subsequently for confluency [ii] Phase contrast image of RAPC in monolayer on fibronectin-coated plates show a stellate body with cell progeny emanating from a central colony (scale bar =50micrometers) [iii] DiI fluorescence of RAPC after 6 hour exposure to DiI-ac-(human) LDL (scale bar =10micrometers) [iv] composite image (80μ depth) of RAPC treated with VEGF exhibiting capillary loop structures in matrigel media (scale bar =50micrometers) (D) Relative CD184, CD309, Sox2, and Oct4 mRNA expression by quantitative PCR in RAPC (n=10 separate patients), human iPS (n=10), human endothelial cells (EC) (n=10), and human aorta-derived vascular smooth muscle cells (VSMC)(n=10) (4 groups compared pairwise); CD184, RAPC vs iPS

(1.00±0.00 vs 0.12±0.20)(*p<0.001, CI=0.77–1.03); CD184, RAPC vs EC (1.00±0.00 vs 0.02±0.00)(**, p<0.001, CI=0.76–1.01); CD184, RAPC vs VSMC (1.00±0.00 vs 0.046±0.03)(***, p<0.001, CI=0.86–1.12); CD309, RAPC vs iPS (1.00±0.00 vs 0.04±0.03)(*p<0.001, CI=0.89–1.02); CD309, RAPC vs EC (1.00±0.00 vs 0.11±0.02)(**, p<0.001, CI=0.83–0.96); CD309, RAPC vs VSMC (1.00±0.00 vs 0.04±0.03)(***, p<0.001, CI=0.93–1.06); Sox2, RAPC vs iPS (1.00±0.00 vs 1.02±0.13)(p=NS, CI=−0.06–1.0); Sox2, RAPC vs EC (1.00±0.00 vs 0.03±0.02)(*, p<0.001, CI=0.88–1.05); Sox2, RAPC vs VSMC (1.00±0.00 vs 0.00±0.00)(**, p<0.001, CI=0.91–1.08); Oct4, RAPC vs iPS (1.00±0.00 vs 1.04±0.10)(p=NS, CI=−0.11–0.03); Oct4, RAPC vs EC (1.00±0.00 vs 0.04±0.05)(*, p<0.001, CI=0.89–1.02); Oct4, RAPC vs VSMC (1.00±0.00 vs 0.00±0.00)(**, p<0.001, CI=0.93–1.06).

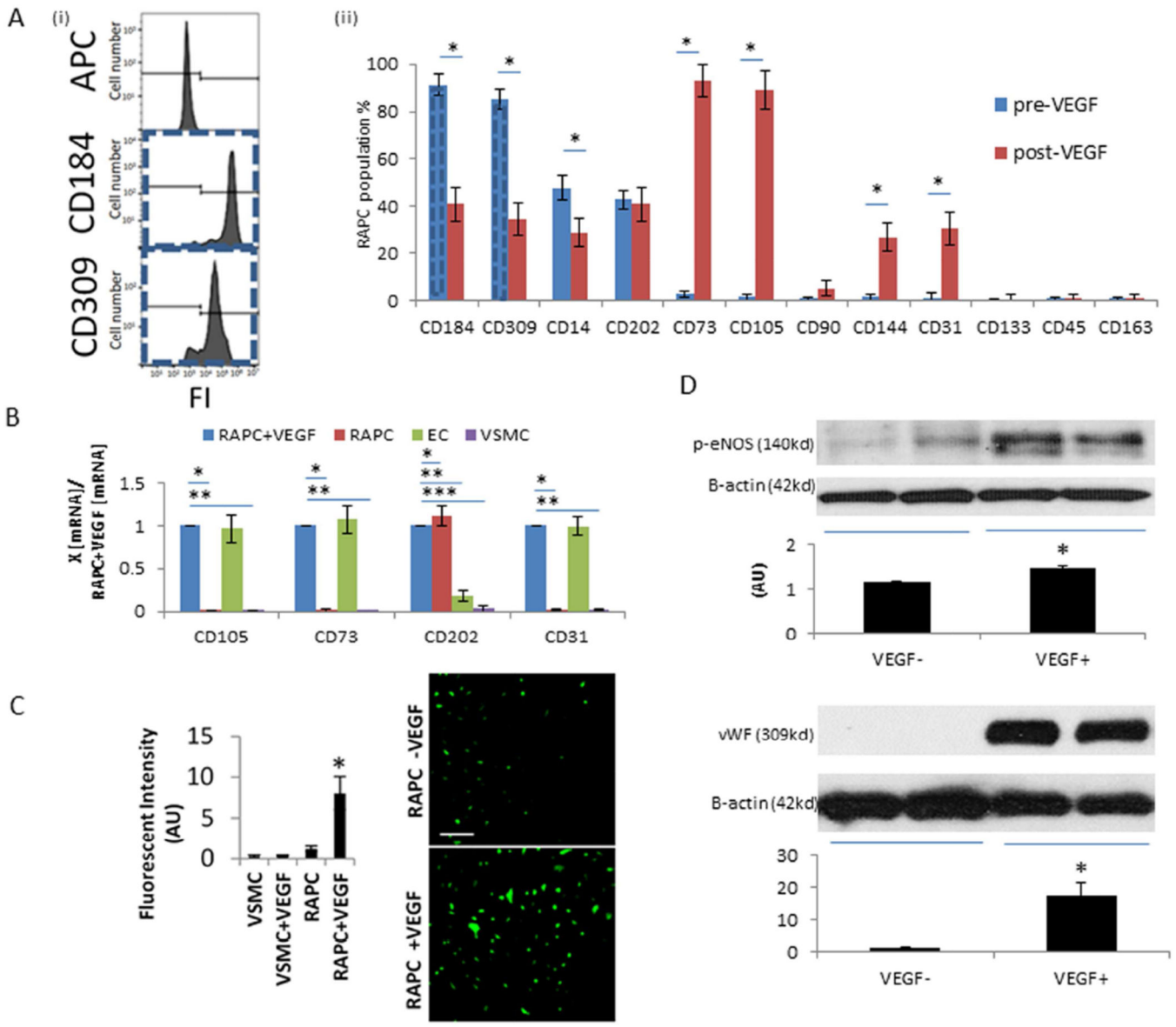

Figure 3.

Characterization of renal artery-derived progenitor cell culture (A)[i] Isolation of RAPC by single-cell sorting. Representative fluorescent intensity (FI) histogram due to binding of non-specific IgG2a-κ isotype control control antibody (0.0%), anti-human CD184 monoclonal antibody labelled with APC (94.7%) and anti-human CD309 antibody labelled with APC (85.3%) on sorted cells derived from non-confluent monolayer prior to VEGF exposure (dashed line linked to CD184 and CD309 bar graph), cell count=10,000 per condition, [ii] RAPC cultured for seven days in basal media compared to RAPC treated with VEGF (n=22), CD184 pre- vs post-VEGF (91.3±4.3%, vs 37.0±5.2%), CD309 pre- vs post-VEGF (85.2±4.3% vs 34.6±4.2%), CD14 pre- vs post-VEGF (48.0±5.1% vs 27.6±4.58%), CD202 pre- vs post-VEGF (42.9±4.0% vs 38.4±4.0%), CD73 pre- vs post-VEGF (2.9±1.2% vs91.5%±3.8%), CD105 pre- vs post-VEGF (1.5±1.3 vs 88.9±4.5%), CD90 pre- vs post-VEGF (0.8±0.7% vs 2.6±1.9%), CD144 pre- vs post-VEGF (1.6±1.3% vs 27.7±3.9), CD31

(1.4±1.8% vs 29.2±3.2%), CD133 pre- vs post-VEGF (0.5±0.6% vs 0.96±1.1), CD45 (0.9±0.8% vs 0.6±0.9%) CD163 (0.8% ± 0.9%), respectively; (*, p<0.001). (B) Relative CD105, CD73, CD202, and CD31 mRNA expression by quantitative PCR in RAPC+VEGF (n=10 separate patients), RAPC (n=10 separate patients), human EC (n=10) and human VSMC (n=10) (4 groups compared pairwise). CD105, RAPC+VEGF vs RAPC (1.00±0.00 vs 0.01±0.01)(*p<0.001, CI=0.89–1.10); CD105, RAPC+VEGF vs VSMC (1.00±0.00 vs 0.00±0.00)(**, p<0.001, CI=0.89–1.10); CD73, RAPC+VEGF vs RAPC (1.00±0.00 vs 0.01±0.01)(*p<0.001, CI=0.89–1.10); CD73, RAPC+VEGF vs VSMC (1.00±0.00 vs 0.00±0.00)(**, p<0.001, CI=0.89–1.10); CD202, RAPC+VEGF vs RAPC (1.00±0.00 vs 1.11±0.11)(*p=0.002, CI=−0.19–0.03); CD202, RAPC+VEGF vs EC (1.00±0.00 vs 0.18±0.06)(**, p<0.001, CI=0.88–1.04); CD202, RAPC+VEGF vs VSMC (1.00±0.00 vs 0.04±0.04)(***, p<0.001, CI=0.89–1.10); CD31, RAPC+VEGF vs RAPC (1.00±0.00 vs 0.02±0.01)(*p=0.001, CI=−0.91–1.04); CD31, RAPC+VEGF vs VSMC (1.00±0.00 vs 0.02±0.01)(**, p<0.001, CI=0.91–1.05); (C) Fluorescent intensity (arbitrary units, AU) of trazolofluorescein was measured to assess for NOS activity, before (RAPC) and after (RAPC +VEGF) VEGF exposure (1.16±0.35 [AU][n=10] vs 8.05±2.03 [n=10]; *, p<0.001). NOS was also measured in human vascular smooth muscle cells (scale bar = 200 micrometers). (D) Representative immunoblots of eNOS (1.16 ± 0.02 AU [n=7] vs 1.48 ± 0.07 [n=7]; p=0.01) and vWF protein (1.10± 0.04 [n=8] vs 17.70 ± 3.71 [n=8]; p<0.001) protein expression in RAPC cultured without VEGF supplementation and 7 days after VEGF supplementation, respectively.

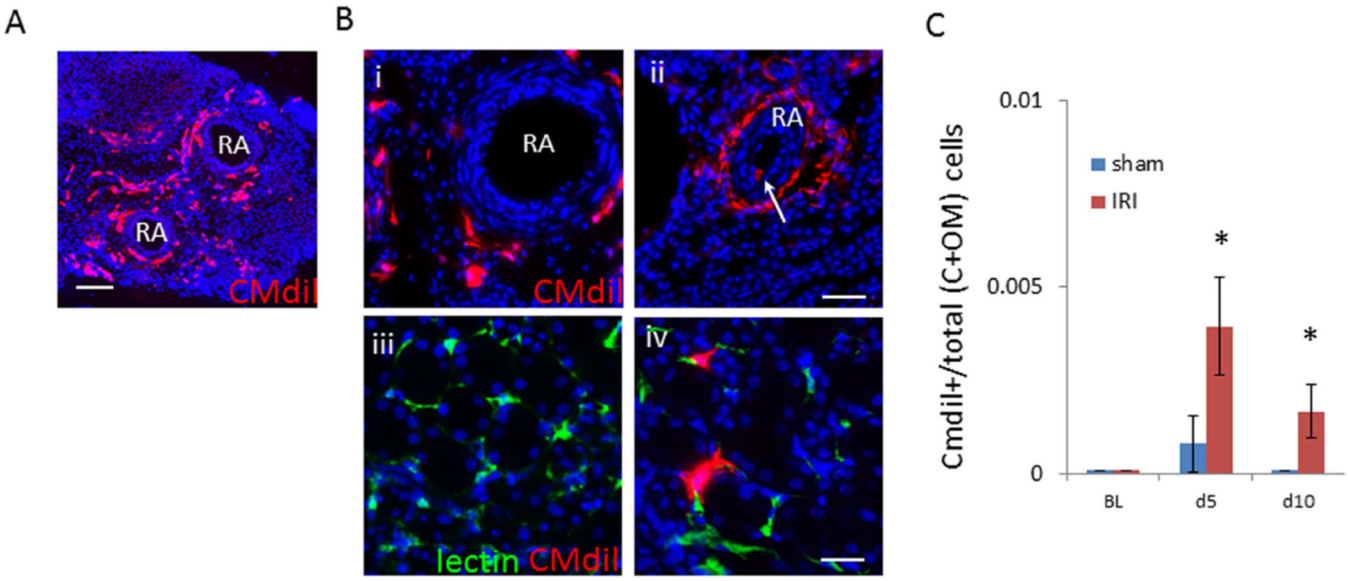

Figure 4.

Cell transit from adventitia of mouse renal artery to kidney parenchyma. (A) CMdil content of adventitia two days after directed injection and IRI (scale bar=500micrometers). (B) CMdil content of renal artery 10 days after [i] CMdil injection and sham injury, [ii] CMdil injection +IRI with CMdil+ cell in vessel lumen (white arrow), and representative image of CMdil content in outer medulla 10 days after [iii] sham and [iv] IRI (low power scale bar=100micrometers, high power scale bar=50micrometers). (C) Total number of CMdil-containing cells among total cells in cortex and outer medulla 5 days after sham (n=5)(0.8 per 1000 cells±0.001) compared to IRI (n=5)(4 per 1000 cells±0.001) (*, $p<0.001$) and 10 days after sham (n=5)(0.1 per 1000 cells±0.000) compared to IRI (n=5)(2 per 1000 cells ±0.001) (*, $p<0.001$)

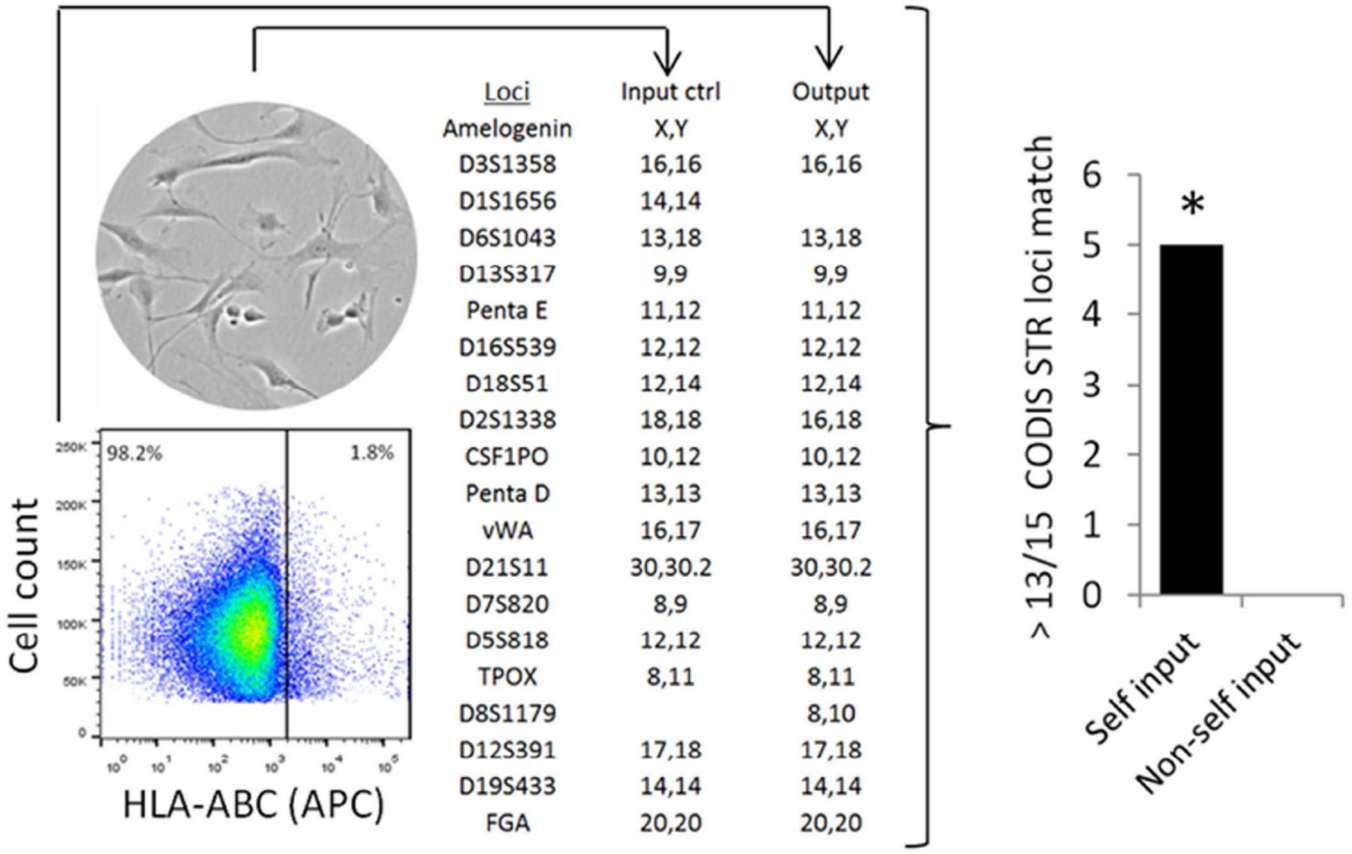

Figure 5.

RAPC are present in an animal model of acute ischemia/reperfusion injury. Near-sconfluent cells were prepared (input control) and injected into NOD/ShiLtSz-*Prkdc*^{scid} animals after undergoing acute renal ischemia/reperfusion injury. 10 days subsequent to injection kidneys were procured and digested. Single cells were probed with HLA-ABC monoclonal antibody (cy3 secondary) to identify the presence of an epitope in the human β-microglobulin subunit (HLA) on cell membranes. Sorted HLA^{+} cells were plated and genomic DNA was extracted (output). A representative comparison of short tandem repeat polymorphisms in 15 consensus loci were analyzed to determine the human origin of cells initially injected into the animal model (input control vs output). DNA from sorted cells (n=5,5) were analyzed in comparison to isolated DNA from the autologous input colony (n=5) and non-autologous input colony derived from other patients (n=5). Each autologous input matched autologous output in 13 of 15 loci (random match probability, $p<1\times10^{-15}$ per paired match analysis).

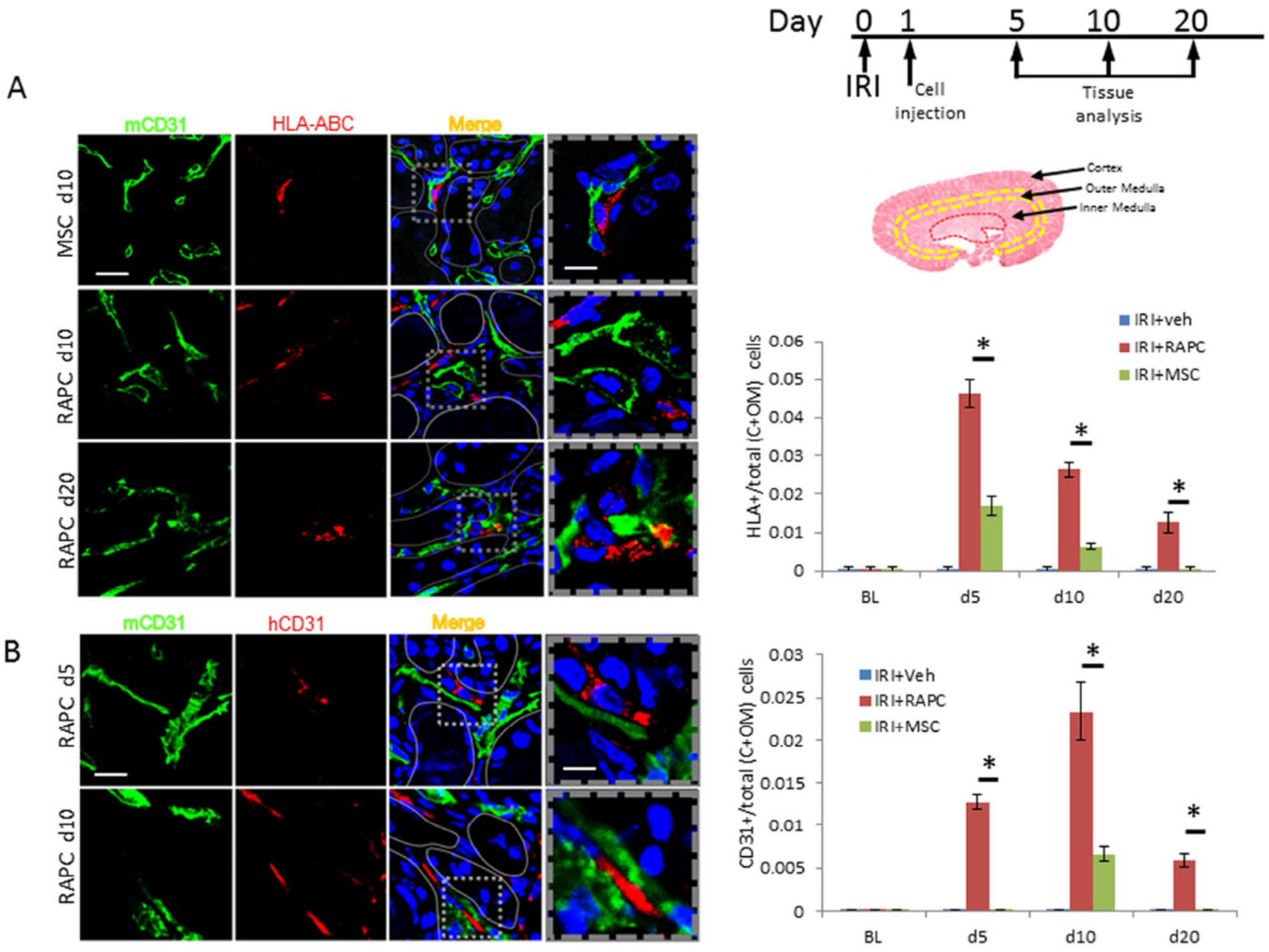

Figure 6.

HLA-ABC-expressing cells and human CD31-expressing cells after RAPC injection. (A) HLA-ABC$^+$ in in the cortex (*C*) and outer medulla (*OM*) compared to total cells (per 10hpf) 5, 10 and 20days after ischemia/reperfusion injury. Photomicrographs are representative of cell density in the outer medulla. RAPC were present in C+OM at 5, 10 and 20 days after IRI showing localization of HLA-ABC adjacent to cells expressing mouse CD31 surface antigen. Fraction of CD31$^+$ to total cells 5 days after injury in RAPC-treated (IRI+RAPC) and MSC-treated (IRI+MSC), respectively (0.046±0.004 [n=7] vs 0.017±0.002 [n=7]; *, p<0.001 [3 groups compared pairwise, CI 0.027–0.041]), and 10 days in IRI+RAPC vs IRI +MSC (0.026±0.002 [n=7] vs 0.006±0.001 [n=7]; *, p<0.001 [CI 0.019–0.024]), and 20 days in IRI+RAPC vs IRI+MSC (0.013±0.003 [n=7] vs 0.000±0.000 [n=7]; *, p<0.001 [CI 0.104–0.147]) (low power scale bar=50micrometers; high power scale bar=25micrometers). (B) Kidney was probed simultaneously for mouse CD31 antigen and human CD31 antigen with monoclonal antibodies. Fraction of human CD31$^+$ cells per total cells in cortex and outer medulla was calculated for tissue 5 days after injury, IRI+RAPC vs IRI+MSC respectively (0.013±0.001 [n=7] vs 0.000±0.000 [n=7]; *, p<0.001, [3 groups compared pairwise, CI 0.012±0.013]), after 10 days, IRI+RAPC vs IRI+MSC (0.023±0.004 [n=8] vs 0.007±0.001 [n=8]; *, p<0.001 [CI 0.014–0.019]), and after 20 days, IRI+RAPC vs IRI

+MSC (0.006±0.001 [n=7] vs 0.000±0.000; *, p<0.001 [CI 0.006–0.007]) (low power scale bar=50micrometers; high power scale bar=10micrometers).

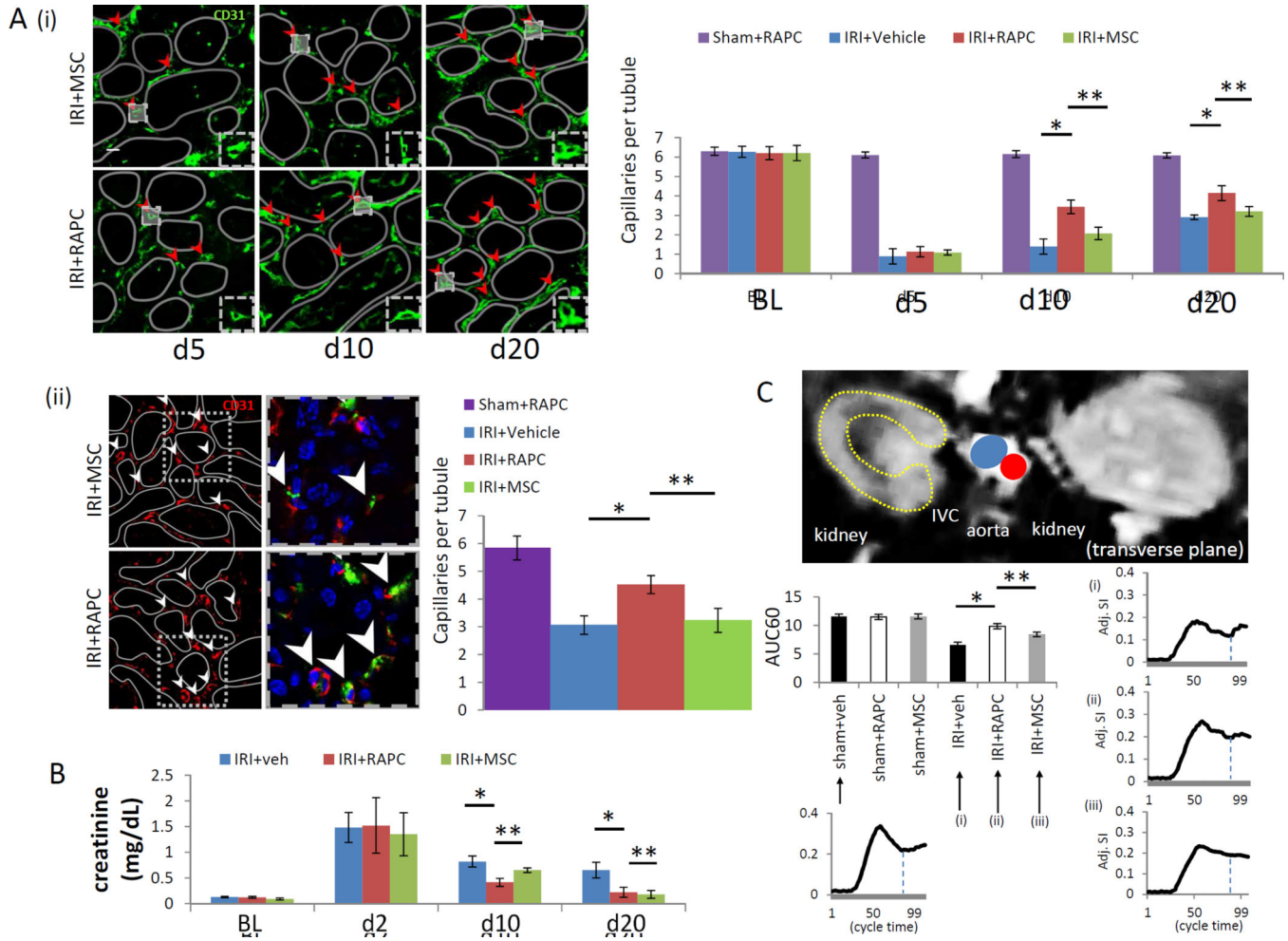

Figure 7.

Functional analysis of RAPC injected after ischemia/reperfusion injury. (A)[i] Patent peritubular capillary cross sections (red arrowheads) at baseline (BL), five days, ten days and twenty days after ischemia/reperfusion injury. 10 days after injury, IRI+RAPC vs IRI+veh (3.44±0.26 [n=6] vs. 1.40±0.39 [n=6]; *, p=0.016, [4 groups compared pairwise, CI 1.47–2.61]), IRI+RAPC vs IRI+MSC (3.44±0.26 [n=6] vs 2.07±0.13 [n=6]; *, p<0.001 [CI 0.79–1.95]) and, 20 days after injury, IRI+RAPC vs IRI+veh (4.14±0.39 [n=6] vs 2.90±0.12 [n=6]; *, p<0.001 [CI 0.78–1.71]), IRI+RAPC vs IRI+MSC (4.14±0.39 vs 3.20±0.35 [n=6]; **, p<0.001 [CI 0.48–1.39]) respectively, (low power scale bar=50micrometers; high power scale bar=20micrometers) [ii] Capillary quantification (peritubular capillaries per tubular lumen) via fluosphere nanoparticle injection 20 days after injury, IRI+RAPC vs IRI+veh (4.52±0.34 [n=5] vs 3.06±0.43 [n=5]; *, p=0.005 [CI 0.31–2.09]), IRI+RAPC vs IRI+MSC (3.22±0.32 [n=5]; **, p=0.03 [CI 0.04–2.01]) (low power scale bar=50micrometers; high power scale bar=10micrometers). (B) Serum creatinine in animals 10 days after injury in IRI +RAPC vs IRI+veh (0.41±0.08 [n=6] vs 0.85±0.12 [n=6]; *, p<0.001, CI −0.56 to −0.30), IRI+RAPC vs IRI+MSC (0.41±0.08 [n=6] vs 0.65±0.04 [n=6]; **, p=0.001, CI −0.37 to −0.11), and 20 days after injury, IRI+RAPC vs IRI+veh (0.21±0.01 [n=6] vs 0.65±0.02 [n=6]; *, p<0.001, CI −0.62 to −0.27), and IRI+RAPC vs IRI+MSC (0.21±0.01 [n=6] vs

0.18±0.08 [n=6]; p=NS) respectively. (C) Gadolinium contrast intensity (arbitrary units) over initial 60% of time interval (AUC60) obtained by DCE-MRI in animals 20 days after IRI, comparing IRI+RAPC vs IRI+veh (9.84±0.46 [n=5] vs. 6.57±0.47 [n=5]; *, p<0.001 [6 groups compared pairwise, CI 2.36–4.18]) IRI+RAPC vs IRI+MSC (9.84±0.46 [n=5] vs 8.42±0.40 [n=5]; **, p=0.001, CI 0.50–2.33) and respectively.

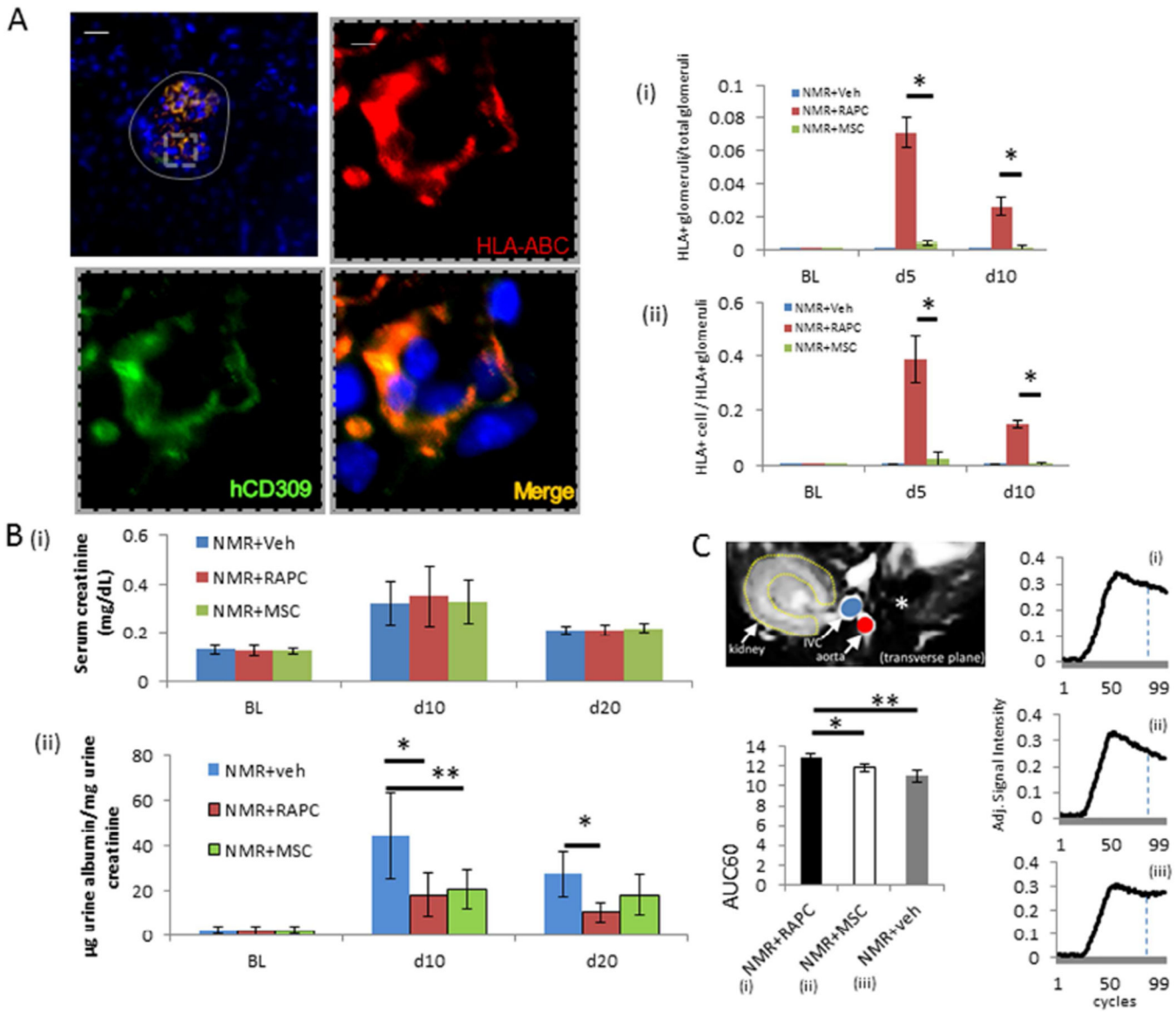

Figure 8.

Histologic characterization and functional analysis of RAPC injected after nephron mass reduction. (A) glomerular content [grey solid line] of HLA in animals treated with RAPC (n=7 per group per time point) (low power scale bar=75micrometers; inset (dashed line), high power scale bar=10micrometers). (i) Fraction of HLA+ glomeruli per total glomeruli 5 days after injury, NMR+RAPC vs NMR+MSC (0.071±0.009 vs 0.004±0.001; *, p<0.001 [3 groups compared, CI 0.060–0.075]) and 10 days after injury, NMR+RAPC vs NMR+MSC (0.026±0.009 vs 0.0±0.0; *, p<0.001 [CI 0.018–0.027]) (scale bar=50micrometers; inset scale bar=10micrometers) (ii) Fraction of HLA+ cells per glomerulus 5 days after injury, NMR+RAPC vs NMR+MSC (0.389±0.090 vs 0.024±0.009; *, p<0.001 [3 groups compared, CI 0.291–0.439]) and 10 days after injury, NMR+RAPC vs NMR+MSC (0.149±0.011 vs 0.005±0.005; *, p<0.001 [CI 0.135–0.154]) respectively. (B) (i) Serum creatinine 10 days after nephron mass reduction (n=8 per group) (3 groups compared

pairwise), NMR+veh (0.32±0.09), NMR+RAPC (0.35±0.12mg/dL), NMR+MSC (0.33±0.09), and after 20 days NMR+RAPC (0.21±0.02) and NMR+MSC (0.22±0.02) and NMR+veh (0.21±0.02), (ii) ratio of urinary microalbumin (μg) to urinary creatinine (mg) after 10 days, NMR+veh vs NMR+RAPC (44.6±19.2μg/mg [n=8] vs 18.2±9.4 [n=8]; *, p=0.002 [3 groups compared, CI 8.8–43.2]), NMR+veh vs NMR+MSC (20.5±8.4; **, p<0.001 [CI 6.4–40.8]), and 20 days, NMR+veh vs NMR+RAPC (27.4±9.9 [n=8] vs 10.3±4.8 [n=8]; *, p=0.002 [CI 6.1–28.0]) respectively. (C) Gadolinium contrast intensity (arbitrary units) over initial 60% of time interval (AUC60) obtained by DCE-MRI in animals 20 days after NMR, comparing NMR+RAPC vs NMR +MSC (12.89±0.41 [n=5] vs 11.88±0.37 [n=5]; *, p=0.025 [3 groups compared pairwise, CI 0.12–11.89]) and NMR +RAPC vs NMR +veh (12.89±0.41 [n=5] vs 10.99±0.67 [n=5]; **, p<0.001 [CI 1.01–2.78]) respectively.

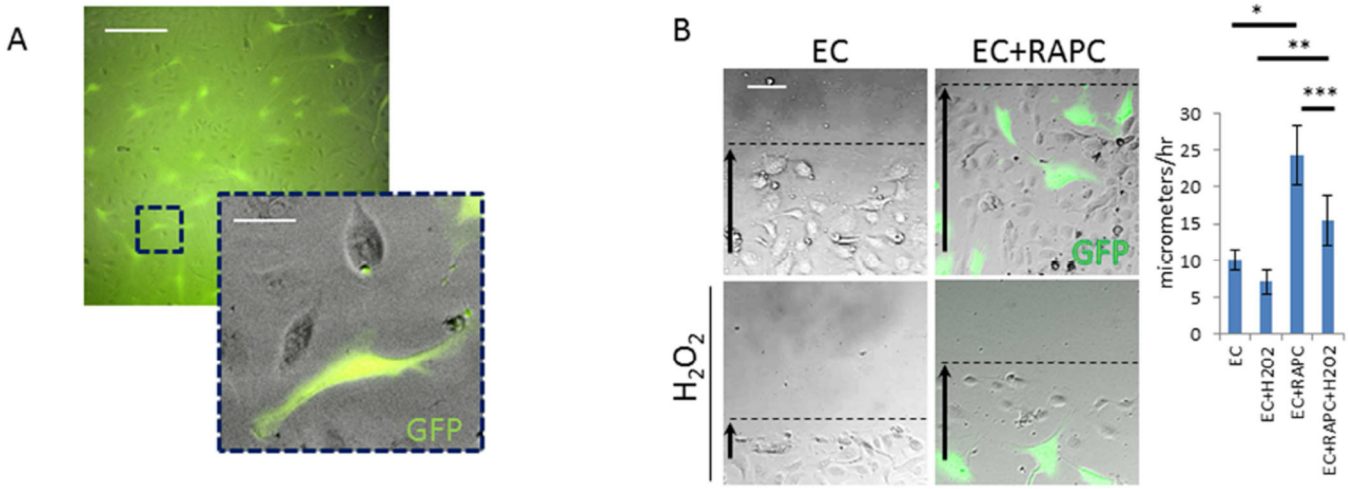

Figure 9.

RAPC promote endothelial survival and migration after hydrogen peroxide-induced endothelial injury. (A) GFP-transfected RAPC could be grown in co-culture with differentiated human endothelial cells. (scale bar = 100micrometers, scale bar inset = 25 micrometers), (B) Representative photomicrograph 13 hours after denudation. Rate of migration in EC+veh (saline) vs EC+RAPC+veh (n=9 per condition, 5 groups compared pairwise) (10.0±1.3micrometers/hr vs 24.4±4.1micrometers/hr; *, $p<0.001$, [CI=−18.7 to −10.0]), EC+H_2O_2 vs EC+RAPC +H_2O_2 (7.0±1. vs 15.5±3.4; **, $p<0.001$, [CI=−21.7–13.0]) and EC+RAPC+H_2O_2 vs EC+RAPC+veh (***, $p<0.001$, [CI=−13.2 to −4.6]) respectively (scale bar = 80micrometers).

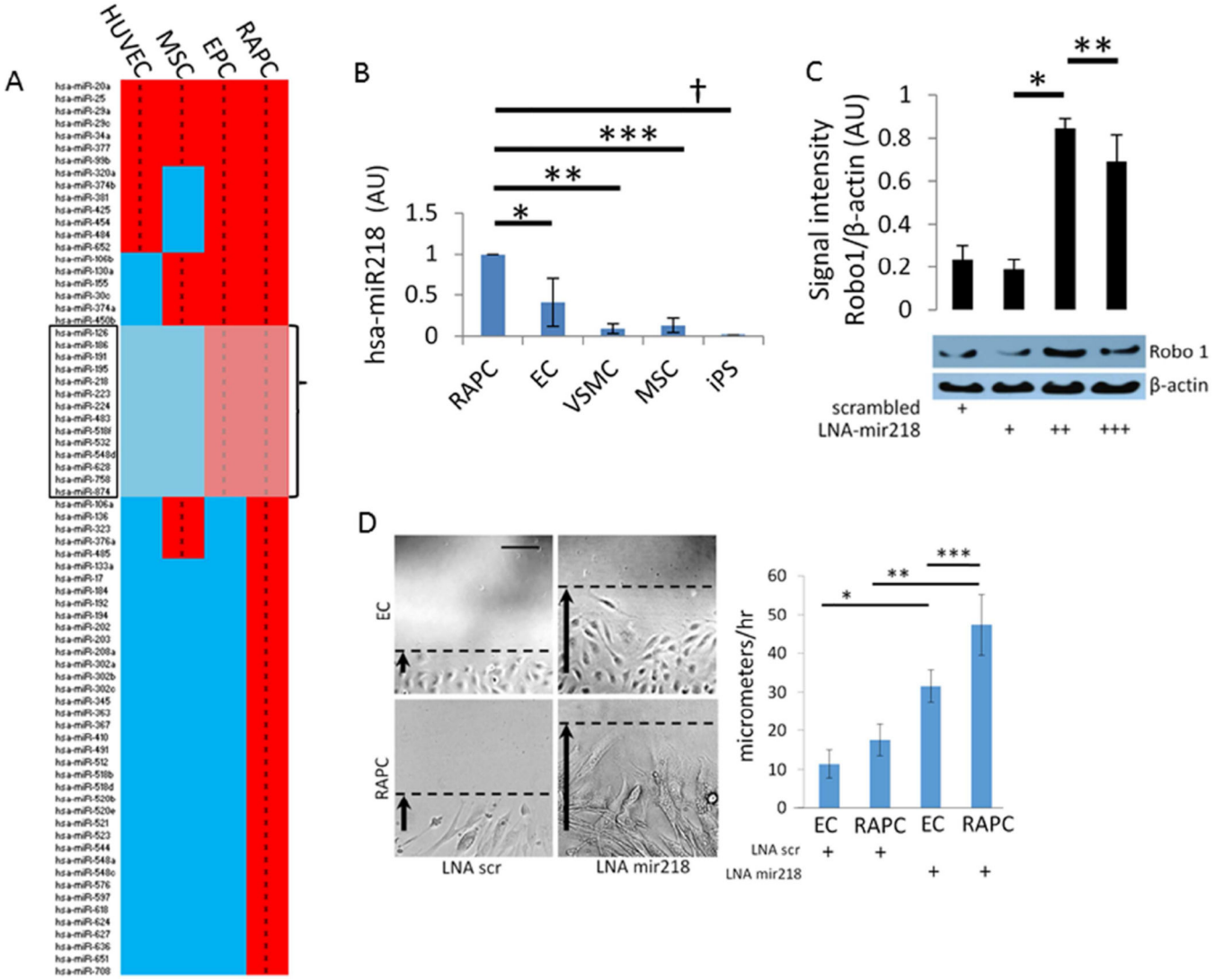

Figure 10.

mir218 expression in human RAPC (A) 73 miRNA were detected from freshly isolated RAPC (n=4). miRNA expression detected in all samples was compared to EPC (n=3), MSC (n=3), and HUVEC (n=3) to calculate Pearson's ρ coefficient in relation to RAPC miRNA expression. Correlation coefficients compared RAPC to EPC miRNA expression (0.67, CI 0.54–0.79; p<0.01), to MSC (0.51, CI 0.32–0.66; p<0.01) or HUVEC (0.36, CI 0.14–0.54; p<0.01). (B) mir-218 expression in cell types compared to RAPC (n=6 experiments per group) (5 groups compared pairwise). RAPC vs EC (0.41±0.29; *, p<0.001 [CI, 0.345–0.834]), vs VSMC (0.091±0.06; **, p<0.001 [CI, 0.67–1.15], vs MSC (0.13±0.09; ***, p<0.001 [CI 0.62–1.11], vs iPS (0.01±0.01; †, p<0.001 [CI, 0.75–1.24]. (C) RAPC treated with scrambled LNA, 12.5, 25, and 100 nM mir-218 LNA (n=10 per group) (4 groups compared pairwise). Normalized signal intensity (arbitrary units), 12.5nM vs 25nM (0.18±0.05 vs 0.85±0.04; *, p<0.001, [CI −0.75 to −0.56]), 25nM vs 100nM (0.85±0.04 vs 0.69±0.13; **, p<0.001, [CI 0.06–0.25]). (D) Cell migration in RAPC and EC after mir-218 inhibition (n=9 experiments per group) (4 groups compared pairwise). Cells were pre-treated

with 50nM LNA scrambled or LNA mir-218 and monitored for migration after linear denudation. Photomicrographs are representative of conditions 6.5 hours after manual denudation. Rate of migration (micrometers/hour) of EC+LNA mir218 was compared to EC +LNA scr (31.5±4.1 vs 11.4±3.4; [CI 12.5–27.7]; *, $p<0.001$) respectively; RAPC+LNA mir218 was compared to RAPC treated with scrambled LNA (49.5±2.6 vs 15.5±4.2; **, $p<0.001$, [CI 21.3–32.7]) respectively, and RAPC+LNA mir218 was compared to EC treated with LNA mir218 (31.5±4.1) (**, $p<0.001$, [CI 8.4–23.2]) respectively (scale bar =100micrometers).

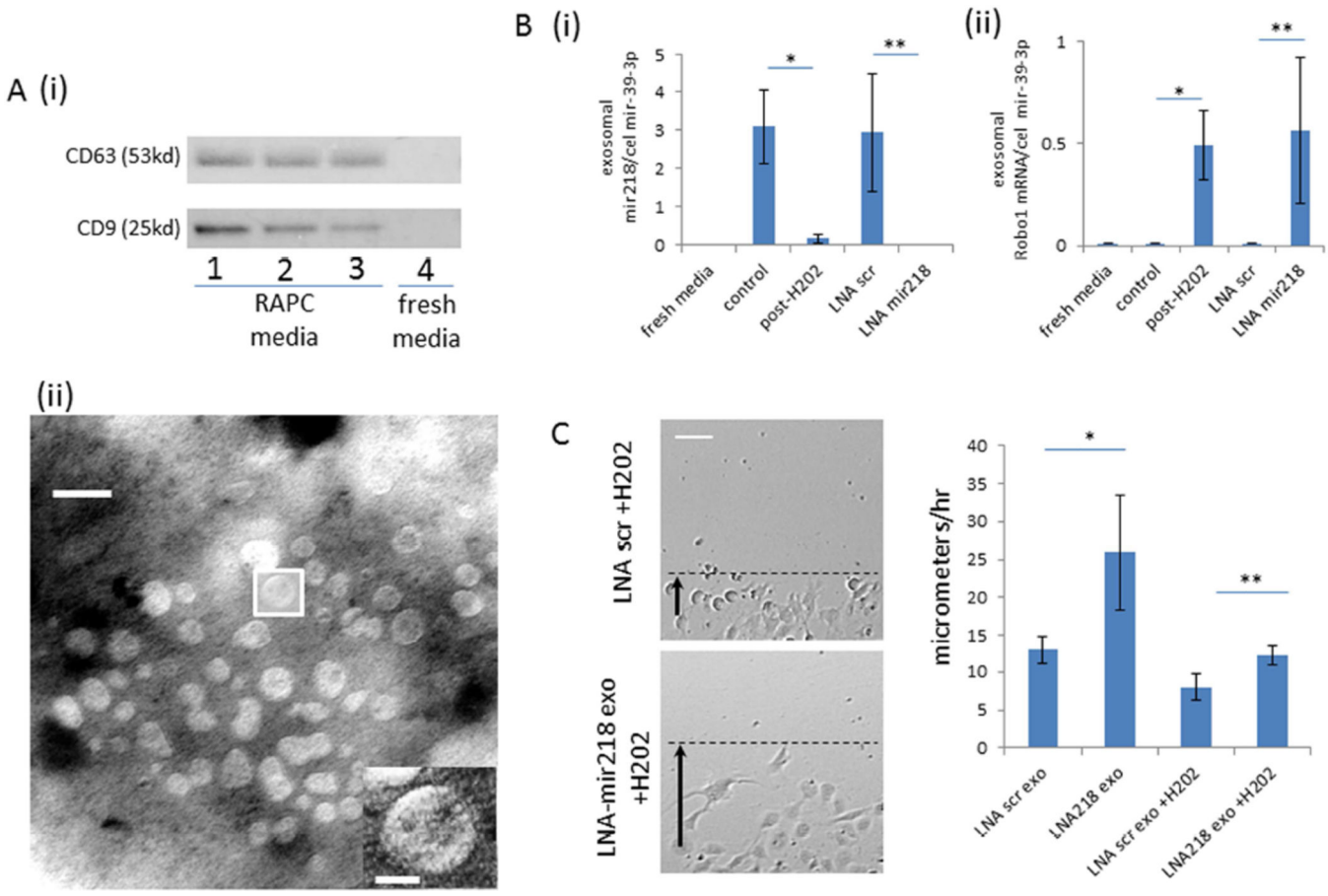

Figure 11.

Characterization of exosomes in RAPC following oxidant stress (A) [i] immunoblot of enriched exosome isolates probed for CD63 and CD9 protein expression from fresh media exposed to RAPC (lanes 1–3 derived from three separate patients) and fresh media not in contact with cells (lane 4), [ii] electron microscopy image of exosomes extracted from agar preparation (scale bar = 30 nanometers). (B)[i] Ratio of RAPC exosomal expression of mir-218 to cel-mir-39 (mean triplicate values from four separate patients, n=4 per group)(5 groups compared pairwise), control vs post-H_20_2 (3.102 ±0.960 vs 0.174±0.127 [CI 0.968–4.889]; *, p=0.002), LNA scr vs LNA mir218 (2.951±1.539 vs 0.001±0.001 [CI 0.991–4.911; **, p=0.002) [ii] Ratio of exosomal Robo-1 mRNA expression to cel-mir-39 (mean triplicate values from four separate patients, n=4 per group)(5 groups compared pairwise), control vs post-H_20_2 (0.001±0.002 vs 0.491±0.167 [CI −0.916 to −0.70]; *, p=0.016), LNA scr vs LNA mir218 (0.564±0.358 vs 0.002±0.002 [CI −1.017 to −0.111]; **, p=0.012) respectively (C) Migration of injured endothelial cells after treatment with exosomes isolated from RAPC+LNA-mir218 (n=4 per group, 5 groups compared pairwise). Rate of migration in LNA scr exo vs LNA 218 exo (n=5 per group) (13.0±1.8micrometers/hr vs 25.9±7.6micrometers/hr; *, p<0.001, [CI=−20.7 to −5.3]), LNA scr exo +H_2O_2 vs LNA 218 exo+H_2O_2 (8.0±1.7 vs 12.2±1.23; **, p<0.001, [CI=6.0–21.5]) respectively (scale bar =80micrometers).